Science Advances

AAAS

advances.sciencemag.org/cgi/content/full/2/11/e1601102/DC1

Supplementary Materials for

Multicolor 3D meta-holography by broadband plasmonic modulation

Xiong Li, Lianwei Chen, Yang Li, Xiaohu Zhang, Mingbo Pu, Zeyu Zhao, Xiaoliang Ma, Yanqin Wang, Minghui Hong, Xiangang Luo

Published 4 November 2016, *Sci. Adv.* **2**, e1601102 (2016)
DOI: 10.1126/sciadv.1601102

The PDF file includes:

Other Supplementary Material for this manuscript includes the following:
(available at advances.sciencemag.org/cgi/content/full/2/11/e1601102/DC1)

- movie S1 (.avi format). The evolution of the images at different elevations above the hologram for “3D imaging.”

section S1. Plasmonic nanoantenna array fabrication. It should be noted that the fabrication parameters are not the same for every design. The details are discussed below respectively:

"Flower" and "map of China"

"Flower" and the "map of China" are designed to appear with different illumination angles. The combined image of these two holographic images is then recorded on the same hologram. The sample is fabricated on 0.635-mm-thick quartz substrates covered with a 75-nm-thick Cr film. The nano-slit antenna arrays are then fabricated on the Cr film using the electron beam lithography (EBL). For this sample, 4000 pixels × 4000 pixels are fabricated on an area of 2 mm × 2 mm. The period for the nano-slit antenna is 500 nm in both the x and y directions. The dimensions of the nano-slit are 300 nm × 150 nm.

Seven-color Hologram

This hologram is fabricated on the same Cr film described in the previous section. For this sample, 1,428 pixels × 1,428 pixels are fabricated on an area of 500 μm × 500 μm. The period for the nano-slit antenna is 350 nm in both the x and y directions. The dimensions of the nano-slit are 250 nm × 100 nm.

Multicolor 3D hologram

For this hologram, the sample is fabricated on 1-mm-thick quartz substrates. A 3-nm-thick Cr film and a 120-nm-thick Au film are subsequently deposited on the cleaned substrates by magnetron sputtering in a same sputter chamber. The sputter deposition rates for Cr and Au are $R_{Cr} \approx 0.83$ nm s^{-1} and $R_{Au} \approx 0.92$ nm s^{-1}, respectively. The nano-slit antenna arrays are then milled on the Au/Cr film using a Ga^+ FIB (FEI Helios NanoLab 650). The period of the nano-slit antenna is 200 nm in both the x and y directions. 150 pixels × 150 pixels are fabricated on an area of 30 μm × 30 μm. The dimensions of the nano-slit are 140 nm × 60 nm.

section S2. Experimental setup of optical characterization. The incident angle is defined in fig. S1. From this figure, we can derive the relations among the incident angles

$$\cos^2(\theta_x)+\cos^2(\theta_y)+\cos^2(\theta_z)=1 \qquad \text{(S1)}$$

For each design, the incident angle is not the same. The details are discussed below. For convenience, only θ_x and θ_y are listed. With the eq. (S1), θ_z can be calculated ($\mathbf{0} < \theta_z < \frac{\pi}{2}$).

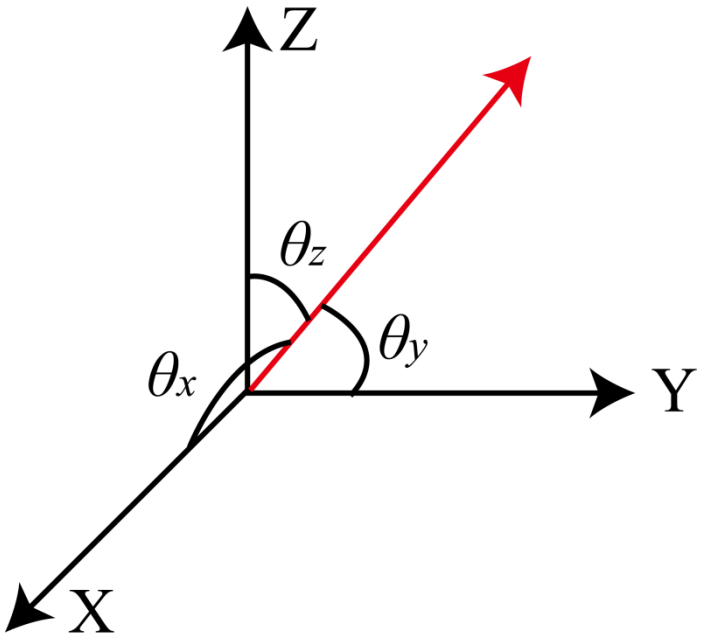

fig. S1. Definition of incident angles. (the normal direction of the hologram surface is in +z direction).

The incident angles for “flower”, “map of China”, “seven-color hologram” and “3D imaging” are shown in table S1, table S2, table S3 and table S4.

table S1. Incident angles for "flower."

Color	θ_x (Degree)	θ_y (Degree)
Red	90-18.45=71.55	90-18.45=71.55
Green	90	90-15.43=74.57
Blue	90+11.68=101.68	90-11.68=78.32

table S2. Incident angles for "map of China."

Color	θ_x (Degree)	θ_y (Degree)
Red	90-18.42=71.58	90
Green	90-15.43=74.57	90
Blue	90-11.68=78.32	90

table S3. Incident angles for "seven-color hologram."

Color	θ_x(Degree)	θ_y (Degree)
Red	90-37.06=52.9	90-37.06=52.94
Orange	90	90-35.52=54.48
Yellow	90+33.86=123.86	90-33.86=56.14
Green	90-30.44=59.56	90
Cyan	90+29.37=119.37	90
Blue	90-26.77=63.23	90+26.77=116.77
Purple	90+22.69=112.69	90+22.69=112.69

table S4. Incident angles for "3D imaging."

Color	θ_x (Degree)	θ_y (Degree)
Red	90-40=50	90
Green	90	90-40=50
Blue	90+15=105	90+30=120

section S3. Simulation results for the seven-color hologram. The simulation results for seven-color holography "Sun Phoenix" pattern is shown in fig. S2. The holographic image is made of red, orange, yellow, green, cyan, blue and purple colors. The experimental results are very similar to the simulation results. The color difference is due to the mismatch between the illumination laser and the real color.

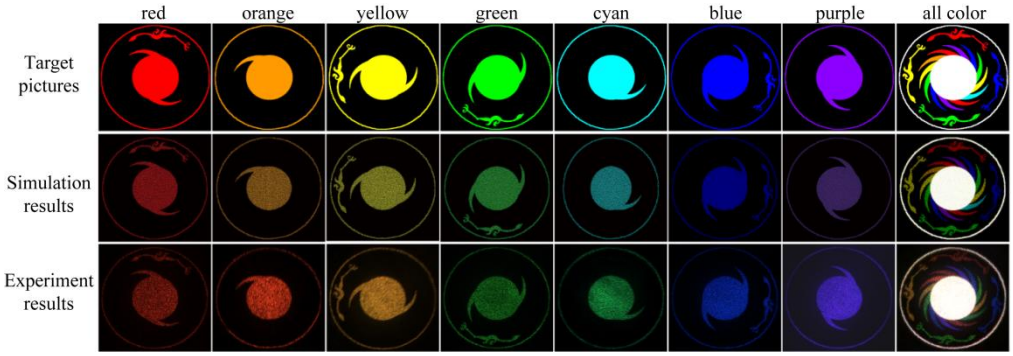

fig. S2. Target pictures, simulation, and experimental results of the seven-color Sun Phoenix holography.

section S4. Calculation of the color gamut. In our experiments, we represent each color with a specific laser. The wavelengths for these lasers are summarized in the table S5. These colors are then plotted into the CIE 1931 color space. The CIE 1931 color space is the quantitative representation of physical pure colors (i.e. wavelengths) in the visible electromagnetic spectrum. Its boundary defines the limit of physiological perceived colors in human color vision. In other words, this color spaces include all

color elements that our eyes can observe. The color gamut is a certain subset in this color space. The areas of the color gamut represent the numbers of colors which can be reproduced and it is an important measurement for the performance of the display devices.

For each wavelength, its corresponding 1931 CIE (*x*, *y*) chromaticity coordinates are calculated from the spectral power distribution (SPD) of the light source and the CIE color-matching functions. The integral functions give the tristimulus values *X*, *Y* and *Z*

$$X = \int P \cdot x d\lambda \tag{S2}$$

$$Y = \int P \cdot y d\lambda \tag{S3}$$

$$Z = \int P \cdot z d\lambda \tag{S4}$$

where *P* is the SPD of the light source and *x*, *y*, *z* are the CIE color matching functions defined by the International Commission on Illumination. From *X*, *Y* and *Z*, the chromaticity coordinates (*x*, *y*) in the CIE color space can be obtained as follows

$$x = \frac{X}{X + Y + Z} \tag{S5}$$

$$y = \frac{Y}{X + Y + Z} \tag{S6}$$

The results are presented in table S5.

table S5. List of the wavelength versus colors.

Color	Wavelength	CIE *x*	CIE *y*
Red	632.8 nm	0.71148	0.28848
Orange	610 nm	0.66576	0.33401
Yellow	585 nm	0.54479	0.45443
Green	532 nm	0.17024	0.79652
Cyan	510 nm	0.01387	0.75019
Blue	473 nm	0.11581	0.07358
Purple	405 nm	0.17302	0.00478

From the coordinates presented in the table S5, we can calculate the area of the color gamut corresponding to the RGB holography (red, green and blue) and seven-color holography (red, orange, yellow, green, cyan, blue and purple)

$$\frac{Area_{7colors} - Area_{RGB}}{Area_{RGB}} = 39\% \tag{S7}$$

section S5. Efficiency of the meta-hologram. The efficiency for the gold nano-antennas in our experiment is calculated with CST Microwave Studio. The results are summarized in fig. S3.

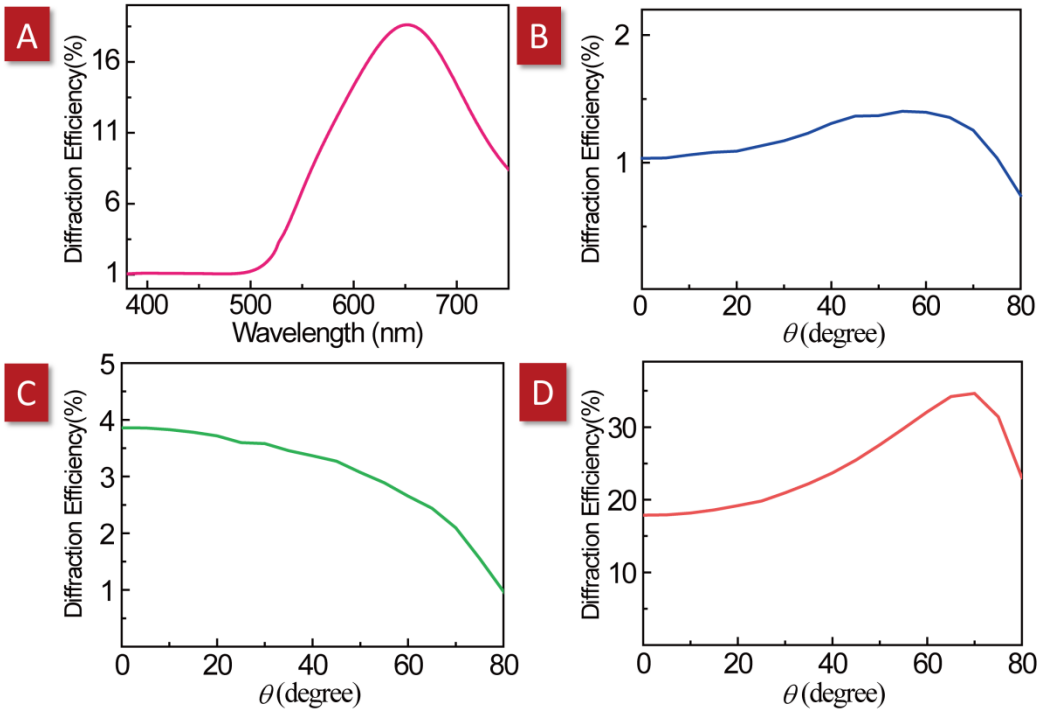

fig. S3. Efficiency of the meta-hologram. A, Efficiency for the gold nano-antenna at different wavelengths (normal incidence); Efficiency at different incident angles for B, 405 nm; C, 532 nm; D, 632.8 nm lasers. The geometry parameters are adopted from our multicolor 3D hologram.

The efficiency is determined by the resonance of the structure as shown in fig. S3A. If we design the structure to resonant for a specific color (wavelength), the efficiency for this wavelength is maximum. When the number of colors increases, the efficiency for

the wavelength beyond the resonance peak will be lower than the resonant one. So the average efficiency of the hologram will be reduced. The efficiency also changes with incident angle for each color, as shown in fig. S3 (B to D). Considering the incident angles of different colors given in table S4, the diffraction efficiencies for red, green and blue are 23.70%, 3.37% and 1.13% respectively. The average diffraction efficiency of our hologram for multicolor 3D meta-holography is 9.4%. It is worth to mention that there is a tradeoff between number of channels we use and efficiency. Because the more colors we use, the more holographic image patterns need to be designed for a single laser source. So the energy needs to be distributed among these patterns. Take into account the energy we can use in the imaging area for 3 primary colors imaging, the absolute efficiency is around 3.13%, which is relatively higher than the multi-color meta-hologram based on resonant scattering (*4*).

The relationship between the number of channels and SNR is related to the algorithm of the holography. For the GS algorithm in calculation of 2D holographic projection, the increase of channel number will not affect the value of SNR. In the GS algorithm we used, the whole imaging plane is divided into N×N pixels in the Fourier space. The increase of the channel number indicates that more pixels are set to non-zero value, while the total number will not change and keep to be N×N. When the termination condition in the iterative process is satisfied, the SNR of single channel image and multi-channel image is almost the same.